FINAL REPORT: ***"Coupling Sorption to Soil Weathering During Reactive Transport: Impacts of Mineral Transformation and Sorbent Aging on Contaminant Speciation and Mobility"*** **(**DE-FG02-06ER64190, 2/15/06-1/31/09). In addition to the five PIs (Chorover, Mueller, O'Day, Serne, Steefel), project personnel include postdoctoral associates Sunkyung Choi (UCM), Aaron Thompson (UA) and Wooyong Um (PNNL), Ph.D. students Nelson Rivera (UCM) and Caleb Strepka (PSU), and research specialist Mary Kay Amistadi (UA).

This project aimed for a predictive-mechanistic understanding of the coupling between mineral weathering and contaminant (Cs, Sr, I) transport/fate in caustic waste-impacted sediments. Based on our prior studies of model clay mineral systems, we postulated that contaminant uptake to Hanford sediments would reflect concurrent adsorption and co-precipitation effects. Our specific objectives were: (1) to assess the molecular-scale mechanisms responsible for time-dependent sequestration of contaminants (Cs, Sr and I) during penetration of waste-induced weathering fronts; (2) to determine the rate and extent of contaminant release from the sorbed state; (3) to develop a reactive transport model based on molecular mechanisms and macroscopic flow experiments [(1) and (2)] that simulates adsorption, aging, and desorption dynamics. Progress toward achieving each of these objectives is discussed below.

1. Molecular-scale mechanisms responsible for time-dependent sequestration of contaminants.
Research has focused on characterization of Hanford sediments reacted with synthetic tank waste leachate (STWL) containing contaminant Cs^+, Sr^{2+} and I^- in batch experiments and comparison to flow-through column experiments. We are using nuclear magnetic resonance (NMR) and Fourier-transform infrared (FTIR) spectroscopies to elucidate mineral transformations during weathering, and coupling those results with synchrotron X-ray absorption spectroscopy (XAS) and extended X-ray absorption fine structure (EXAFS) to determine modes of Sr sequestration in sediments reacted as a function of time. We have established that nitrate-bearing feldspathoid and zeolite phases form with time as a result of sediment reaction with caustic STWL [2]. These secondary phases are capable of taking up both Cs and Sr from solution as they form. Characterization of reaction products by ^{27}Al and ^{29}Si magic angle spinning (MAS) NMR experiments conducted across a range of field strengths at PSU and EMSL have proven extremely useful in determining the time-dependent formation and the relative mass fractions of neophases [4, 5]. EXAFS spectroscopic results also indicate that precipitation of $SrCO_3(s)$ can occur during clay and sediment reaction with STWL if its solubility is exceeded [6]. The fraction of Sr associated with $SrCO_3(s)$, however, is readily removed with mild chemical extraction, and thus represents a labile fraction of Sr, in contrast to the irreversibly-bound fraction associated with neoformed aluminosilicates. Recent investigations are examining conditions that favor the precipitation of labile $SrCO_3(s)$ versus incorporation of Sr and Cs in more recalcitrant, neoformed aluminosilicate phases.

Batch Sediment Studies: Hanford sediments (Hanford course: HC; Hanford fine: HF; Ringhold silt: RG) were reacted for times ranging from 1 h to 369 d in batch aqueous systems with STWL (0.05 *m* $NaAlO_2$, 2.0 *m* Na^+, 1.0 *m* NO_3^- and 1.0 *m* OH^-; pH ~13.7) in the presence of Cs^+ and Sr^{2+}, where both metals were present as co-contaminants at initial aqueous concentrations of 10^{-5},10^{-4} and 10^{-3} m (298 K). At the end of each reaction period, replicates were centrifuged and rinsed in 95% ethanol to remove entrained STWL solution, and either freeze-dried prior to spectroscopic and microscopic analyses or subjected to sequential extraction with 0.1 M $Mg(NO_3)_2$ (a measure of exchangeable Cs or Sr) and 0.2 M acid ammonium oxalate (AAO; a measure of poorly crystalline phases) (see [7-9]for experimental details).

Strontium uptake by all sediments exceeded that of Cs at nearly all reaction times. After 374 d, the total amount of Cs and Sr sorbed in all systems ranged from 15-37% and 80-93% of the initial concentrations, respectively. Although time-dependent trends for Cs uptake were not clearly evident, the fraction of non-exchangeable Cs increased slightly over time despite fluctuations. Strontium became progressively recalcitrant to desorption after 92 d, suggesting that coprecipitation in neoformed phases may be a significant sequestration mechanism for Sr in sediments of the Hanford vadose zone. SEM-EDS showed formation of Cs and Sr containing secondary solid phases after 183 d. Synchrotron μ-XRF and μ-

XRD identified these phases as cancrinite and sodalite. Results indicate that while both Sr and Cs are incorporated into neo-formed precipitates, Sr uptake and lability depends strongly on mineral transformation reactions in the sediments, whereas Cs uptake is strongly influenced by adsorption, probably associated with high-affiinity and edge-sites of native micaceous minerals. Details of experimental conditions and solution-phase chemistry are reported in [2].

^{27}Al and ^{29}Si NMR Studies of Reacted Sediments: Results from ^{29}Si and ^{27}Al magic-angle spinning (MAS) NMR experiments on specimen clay and homogeneous nucleation samples have helped to quantify the time-dependent change in the amount of various Al-bearing secondary solids during the course of reaction under STWL conditions [2, 7, 9, 10]. One-dimensional ^{29}Si and ^{27}Al MAS NMR experiments have been run on unreacted, STWL-reacted, and AAO-extracted HF and RG sediments at all three Cs/Sr co-contaminant concentrations. Figure 1 (two left columns) shows a subset of ^{27}Al MAS NMR spectra of HF sediment samples after 374 d of reaction with STWL containing 10^{-3} *m* Sr and Cs. Spectra were acquired at 21.14 T at the EMSL for the highest possible resolution through reduction of the quadrupolar-induced line broadening; similar data have been acquired from RS sediment samples. These spectra are expanded to show only the region of the spectra that contains resonances from four-coordinate aluminum species, which change markedly as a function of time and treatment. Unreacted HF sediment contains aluminum in tetrahedral coordination, therefore the analysis must take into account the original aluminum present. A detailed mass balance based on initial composition, total spectral intensities, and the deconvolution of the resonances into two or three peaks is in progress. These analyses indicate an increase in resonance intensity attributed to feldspathoid phases (ca. 62 ppm based on earlier studies) after 7 d reaction time. The ratio of the two main peaks (at ca. 62 and 58 ppm) in the four-coordinate Al spectra change from 1.25 in the unreacted sample to 1.62, 1.59, and 1.52 at 7 d, 29 d, and 374 d respectively. The same ratio from the 29 d sample after AAO treatment remains approximately constant (slightly elevated to 1.63), while the mass normalized contribution of these peaks (reflected in the relative intensities for all resonances within each column of Fig. 1) decreases by 9 % with AAO treatment.

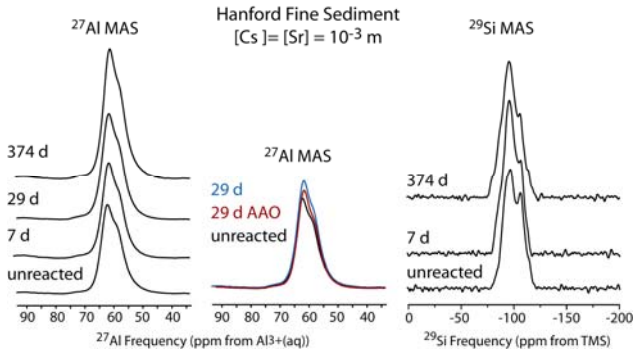

Fig. 1. ^{27}Al and ^{29}Si MAS NMR spectra of unreacted HF sediment and sediment reacted with STWL for up to 374 d (Cs and Sr = 10^{-3} m each) indicate the dissolution of original aluminosilicate phases followed by subsequent neophase formation. Spectra are mass normalized,and therefore allow for a mass-balanced accounting of reaction kinetics including the recalcitrance of neophases (as shown in the center column).

The ^{27}Al MAS analyses are further informed by ^{29}Si MAS NMR data. Figure 1 (right column) contains ^{29}Si MAS NMR spectra of the unreacted and reacted HF samples (10^{-3} *m* Sr+Cs, 7 and 374 d.) The spectrum from the unreacted sample reflects the original complex sediment mineralogy (including quartz and plagioclase indicated by peaks at -110 ppm and in the range of -75 to -105 ppm, respectively), while the reacted samples indicate the changing speciation and relative abundances of silicate species. The quartz phase appears to change little with reaction time, but resonances from the initial plagioclase phases decrease as a function of reaction time, and neophases are introducing new resonances in the same spectral region from -75 to -105 ppm (again consistent with feldspathoid neoformation). Spectral deconvolutions from both ^{27}Al and ^{29}Si NMR data, and employment of correlation analyses combining these and other spectroscopic data, will ultimately describe the complex kinetics of transformation in the sediments, which will then be compared to the uptake and release of contaminant species.

Sr-EXAFS Results for Batch Experiments: All three natural sediments contained native Sr in concentrations that are measurable by EXAFS (HC = 420 ppm; HF = 340 ppm; RG = 170 ppm). For short

equilibration times (1-7 d), native Sr represents a significant fraction of total Sr in the bulk sample since Sr taken up from reactant solutions is between 746-1955 ppm. Thus, the native Sr fraction must be accounted for in the spectra of 7 d reacted samples and 30 d samples extracted with AAO. Quantitative analyses of Sr-EXAFS of unreacted sediments indicate two primary Si/Al distances around Sr in the unreacted sediment (at 3.35 and 3.81 Å), consistent with Sr in the Ca site of plagioclase feldspar[11, 12].

For batch-reacted sediments at 7 d and 33 d, bulk EXAFS spectra (not shown) indicate that Sr from reaction with STWL is incorporated mostly into poorly crystalline, neoformed aluminosilicates, rather than precipitated as $SrCO_3$(s), as seen in the kaolinite system. Backscattering from neoformed phases is overprinted on the Si/Al scattering in the native Sr-bearing phases, which all have second-neighbor Si/Al atoms within a similar range (~3.35 and 3.81 Å). However, constraining interatomic distances from analysis of the unreacted sediments and fitting the remaining spectral features indicates additional Si/Al scattering at slightly different interatomic distances that give rise to cancellation of scattering amplitude.

After one year of reaction, the mass of added Sr incorporated in the solid phase (> 1000 ppm) is much greater than native Sr and thus, the native Sr component was not included in the EXAFS fits. In HC and HF sediments, a fraction of Sr is associated with $SrCO_3$(s) (data not shown). This result is similar to that found in the model clay systems reacted under the same conditions, which show mixtures of $SrCO_3$(s) and neoformed aluminosilicate phases. For illite, $SrCO_3$(s) dominates the EXAFS spectrum, but montmorillonite and vermiculite have different proportions of $SrCO_3$(s) and aluminosilicate neophases. Although $SrCO_3$(s) has a strong spectral signature, it is not the major Sr component in the reacted sediment samples. The $SrCO_3$(s) fraction is easily removed by chemical extraction, as shown by EXAFS analyses of AAO-extracted samples in which no $SrCO_3$(s) is present. The extraction results indicated that 114 ppm and 1163 ppm Sr for one-year HC and HF, respectively, is removed by AAO, placing an upper limit on the amount of Sr associated with $SrCO_3$(s) at ~3% (for HC) and ~30% (for HF) of the total Sr.

In both reacted sediments and model clays, the majority of Sr is associated with neoformed feldspathoid phases after one year, which is best seen in the AAO-extracted samples. The lack of prominent second-neighbor backscattering in the one-year samples compared to unreacted sediments and short-term reacted samples is probably a result of cancellation of scattering paths from Sr bonded in multiple neophases. Bulk XRD, FTIR, and SEM/EDS characterizations confirmed the presence of secondary sodalite and cancrinite, in addition to other unidentified zeolite-type phases, associated with Sr and Cs after 182 d to one year of reaction, and synchrotron microfocused X-ray diffraction data showed Sr was associated with these neoformed solids[13]. Element mapping with synchrotron micro-XRF shows a strong correlation between Sr and Ca in some sediment particles but not in others, and likewise no consistent correlation between Sr and Fe (Fig. 2). These results are consistent with irreversible Sr incorporation into neoformed feldspathoid-type phases, but also show that excess Sr not associated with these phases readily precipitates as $SrCO_3$(s).

2. Contaminant uptake by Hanford sediment in batch and column-flow experiments

Sediments similar in character to those beneath the leaking underground tanks at the DOE Hanford Site were collected from the 218-E-12B Burial Ground excavation site (referred to as Hanford BG). Hanford BG sediments were reacted in both batch and column experiments with STWL in order to (i) compare reaction products with the batch-reacted Hanford sediments (HC, HF, RG) described above; (ii) to examine reaction products in the presence and absence of atmospheric CO_2 reacted for 6 and 12 months in batch reaction; and (iii) to examine uptake and desorption characteristics under flow conditions.

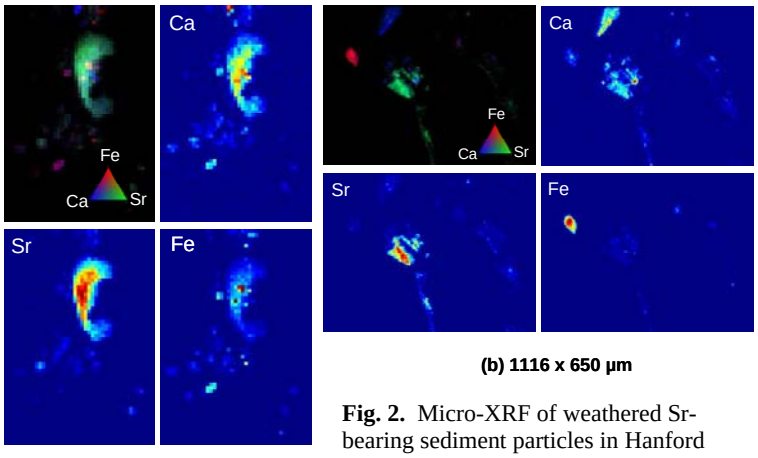

Fig. 2. Micro-XRF of weathered Sr-bearing sediment particles in Hanford sediments after 1 yr reaction.

Hanford BG sediment was reacted with STWL in large batch experiments at high ("H" = 10^{-3} *m* Cs^{+} and Sr^{2+}, 10^{-5} *m* I^{-}) and low ("L" = 10^{-5} *m* Cs^{+} and Sr^{2+}, 10^{-7} *m* I^{-}) contaminant levels at either ambient CO_2 (~383 ppmv) or CO_2-free conditions (undetectable at <10 ppmv within a glovebox). Carboys at ambient CO_2 ('+CO_2') were headspace-flushed with water-saturated air throughout the duration of the experiment. The native sediment contained 150 ± 23 mmol kg^{-1} of inorganic carbon (IC). In the CO_2-free ('–CO_2') treatment 50–70% of this native carbonate was lost in 6 mo, whereas in the '+CO_2' treatments IC concentration increased 10–30%. Uptake of Cs^{+}, Sr^{2+} and I^{-} in these systems is shown in Fig. 3 (no sorption of I^{-} was detected in this case, so it is not shown). Elevated aqueous phase carbonate in the '+CO_2' treatments resulted in the formation of a precipitate along the sidewalls of the carboy in the 'H+CO_2' treatment. This precipitate was high in Sr and inorganic carbon and matched pure standards of $SrCO_3$(s) when analyzed by FTIR and EXAFS (data not shown).

Contaminant sequestration was similar between '–CO_2' and '+CO_2' treatments, however, product solids were different. Both 'H+CO_2' and 'H–CO_2' sediments reacted for 6 months differ spectroscopically from unreacted sediment (data not shown). Sediment treated with 'H+CO_2' resulted in the precipitation of a discrete $SrCO_3$ phase, which is more labile than the secondary aluminosilicate phases. The fraction of Sr is associated with $SrCO_3$(s) was estimated from linear combination fits of the EXAFS at about 20% of the total Sr. The Sr-EXAFS spectrum of 'H–CO_2' sediments shows no evidence of carbonate. Hanford BG sediment reacted for 6 months with low Sr concentrations ('L+CO_2') have a bulk Sr-EXAFS pattern similar to unreacted sediment and show no evidence for the presence of carbonate phases. Quantitative fits indicate slightly longer Sr-Si/Al distances than found for the unreacted sediment (3.42 Å versus 3.35 Å), suggesting the formation of new aluminosilicate phases with a local structure around Sr that differs from native Sr in the sediment.

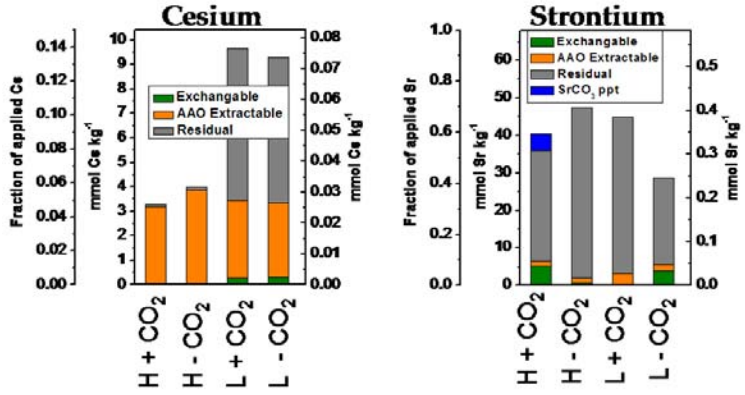

Fig. 3. Distribution of sorbed Cs and Sr (corrected for concentration of Sr in native sediments) among exchangeable, extractable and residual forms following 6 months reaction with STWL in the presence and absence of CO_2. Left Y axis in each figure is for 10^{-3} *m* (H) concentrations; the right Y axis is for the 10^{-5} *m* (L)

Saturated Column Experiments: Flow-through PEEK columns (19 mm I.D. x 76 mm long) were slurry loaded with 34 g of Hanford BG sediment and subjected to stop-flow studies with influent STWL to verify similar modes of Sr sequestration between flow-through and batch experiments. STWL containing 10^{-3} *m* Sr made with N_2-purged water to eliminate CO_2 (but with no other steps to prevent CO_2 from subsequently entering the solution) was pumped into two different columns at 0.69 mL min^{-1} for a total of 12 pore volumes. Flow was stopped for either 1 d (column 1) or 7 d (column 2). Effluent pH was monitored until pH ~12, which occurred at ~2 pore volumes. Column 1 was then flushed with 12 pore

volumes of a synthetic Hanford background pore water solution, whereas column 2 received no flushing. In both cases, the sediment was extruded from the column and dissected into five sections along the length, which were frozen prior to XAS analysis.

Sediment from the outlet end of column 2 (7 d reaction) has a Sr EXAFS spectrum that is similar to that of the native (unreacted) sediment, but with a small reduction in amplitude of the second large peak in the Fourier transform (attributed to scattering from either Si or Al) relative to the first-shell oxygen peak (Fig. 4). In contrast, the EXAFS spectra of sediments taken from the inlet end of both column 2 and column 1 show a much greater reduction in amplitude of the Si/Al peak. These results suggest that STWL-driven weathering reactions proceed quickly at the column inlet, but they tend to neutralize the reactant solution so that much less reaction occurs further down the column. After reaction, the native Sr signal (associated with Sr in feldspar) is overprinted by formation of neophases that have interatomic Sr-Si/Al distances in a range similar to that of the native Sr phase, but with a much larger degree of disorder, resulting in reduction of backscattering amplitude. The results from column experiments are generally similar but not identical to those of previous batch experiments (with HC, HF, and RG described above). Similar reductions in amplitude from Si/Al between reacted and unreacted sediment are apparent, but the interatomic distances derived from fits to the EXAFS are slightly different in the batch-reacted sediments than in the column BG sediments. This may arise either from a different mixture of neoformed phases, or from a different extent of reaction of primary phases, between the batch and column experiments. Data analyses are underway to further characterize the product phases and Sr and Cs sequestration in reacted sediments.

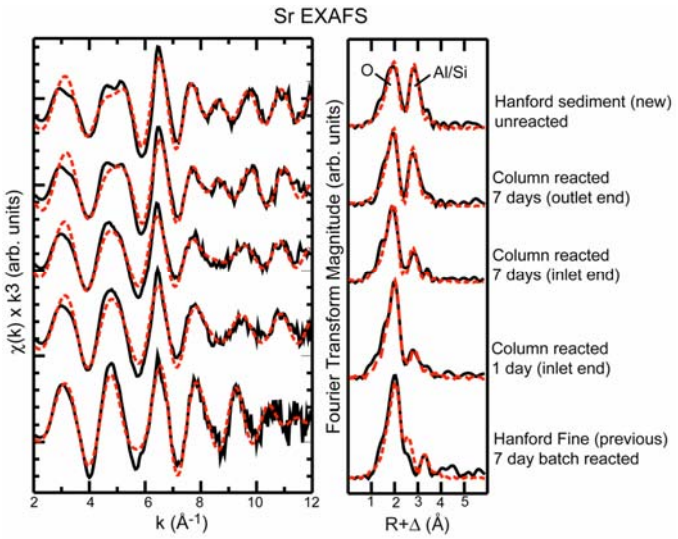

Fig. 4. Sr K edge EXAFS spectra of sediments following 1 or 7 d stopped-flow reaction with STWL.

3. Rate and extent of contaminant release from the sorbed state.

Weathering of Hanford sediments in STWL results in "sorption" of Cs and Sr contaminants into a combination of adsorbed and co-precipitated (including feldspathoid and carbonate) forms, but the stability of these sorbed phases against subsequent desorption and dissolution in background pore waters (i.e., after the caustic source is removed) is not known. Uptake of I^- under these STWL conditions appears minimal. Kinetics of Cs and Sr desorption are being studied in column systems subjected to through-flux of a Hanford background pore-water stimulant. Initial results for the 6 mo. weathered Hanford BG sediments are shown in Fig. 5. Similar patterns are observed for each element at both high and low contaminant loadings. The rate of Cs desorption decreases with time, consistent with release from sites of progressively increasing affinity. In contrast, Sr release is negligible for the first 30-50 pore volumes and then increases significantly, suggesting a threshold in solution undersaturation with respect to a Sr-bearing solid phase, possibly signaling the onset of feldspathoid dissolution. Overall, the data indicate distinctly different desorption dynamics for Sr and Cs that will be pursued in reactive transport modeling. Ongoing and proposed experiments will investigate the effects of porous media saturation, flow rate, stopped flow, and wet-dry cycling on contaminant desorption and neophase transformation kinetics.

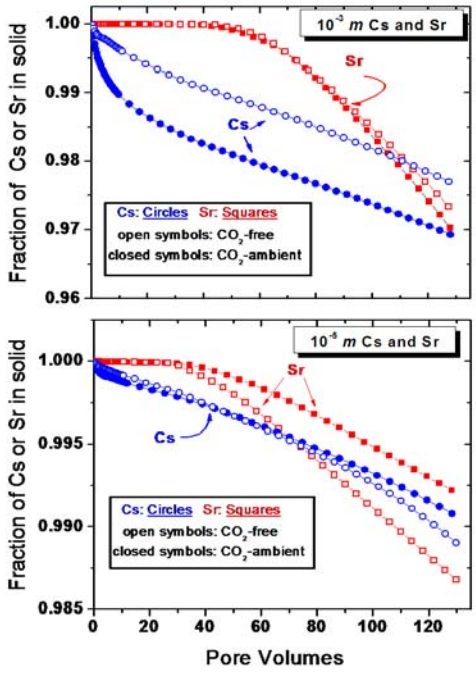

Fig. 5. Column desorption for STWL-weathered sediments subjected to infusion with background pore water (BPW) solutions. Note the distinctly different shapes of the Sr and Cs release curves. Most Sr and Cs appears to be retained in the solid phase even after 120 pore volumes of BPW.

4. Reactive transport modeling.

Flow-through column studies of non-reactive (Br^-) and reactive (Sr, Cs, I) solutes during uptake from STWL and release in BPW are providing a basis for reactive transport modeling. Bromide tracer breakthrough curves show that asymmetry increases with decreasing pore-water saturation, consistent with the presence of immobile regions due to partially filled pores (Fig. 6a). Minor early Br^- breakthrough (~0.92 pore volume at 0.5 C/Co) at 100% saturation is attributed to anion exclusion. When STWL was contacted with quartz sand, Sr retardation exceeded that of Cs and I at both saturation conditions (Fig. 6b). In fact, I^- breakthrough was not significantly different from that of Br^- tracer (data are not shown). There was minor retardation of Cs (R=1.7-2.1), while Sr showed highly retarded transport (R=12.4 and 42.3 for 25% and 37% saturation, respectively). The enhanced retardation of Sr compared to Cs may be due to preferential incorporation of Sr into neoformed aluminosilicate or carbonate precipitates. The fact that greater retardation of Sr occurred at higher water saturation (R=42.3 in 37% saturation) suggests that mineral transformation may have been favored by the greater mineral-STWL contact in the 37% saturated column.

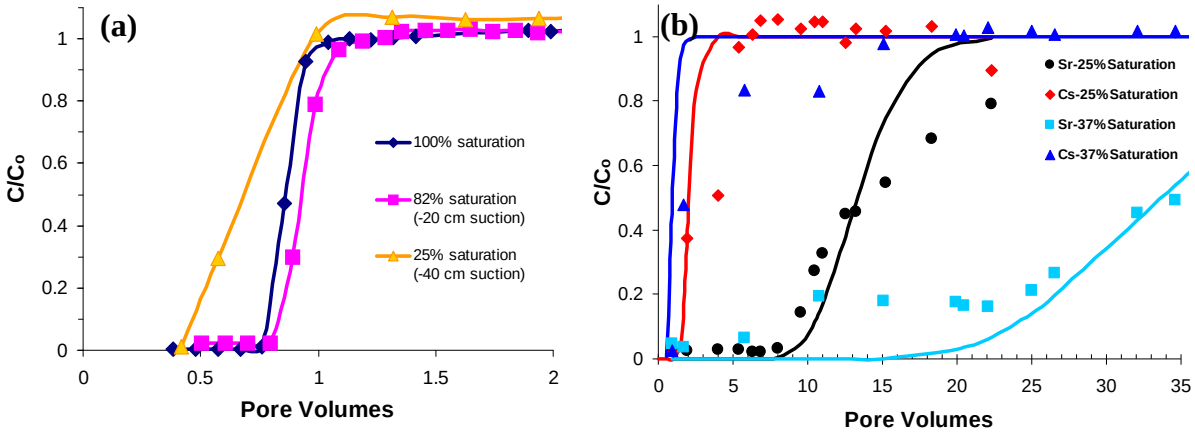

Fig. 6. Breakthrough curves of (a) unreactive Br^- tracer and (b) Sr and Cs as a function of pore saturation. Solid lines are best fits using CXTFIT.

Contaminant desorption from Hanford sediments weathered for times > 6 months is being modeled with the program CrunchFlow. The existing code was modified for this work to accommodate ion exchange in the known neoformed aluminosilicates and validated by matching Cs and Sr desorption using preliminary batch experiments for sediment weathered for 10 months in STWL (Fig. 7). Numerical modeling has confirmed that Cs release does not follow the pattern expected for Cs sorbed to unaltered sediments[1], nor desorption of Cs sequestered by cancrinite[3], but does closely approximate a condition where Cs had been sequestered primarily by sodalite[3]. Based on published Cs exchange capacities for sodalite[3, 14] we estimate that Cs release data could be explained with sodalite comprising less than 10% of the reacted sediment mass. CrunchFlow is now being used to model laboratory column desorption

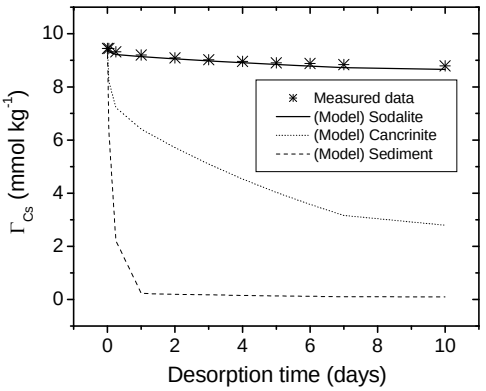

Fig. 7. Desorption of Cs from Hanford fine sediments weathered for 10-months in STWL with 1 mmol Cs/kg soln. Desorption was accomplished in 0.05 M CaCl using a fill/re-fill batch scenario, and the numerical model CRUNCH was adapted to predict desorption under these conditions for the Hanford sediments [1] and for desorption from cancrinite and sodalite [3]. Note the close match between sodalite and the measured data.

experiments (e.g., Fig. 7) to help resolve desorption and dissolution phenomena controlling contaminant release in background pore water.

5. Publications.

Sixteen peer-reviewed publications (including those submitted) have resulted to date from this and prior funding [2, 7-9, 15-29]. Several others are in preparation. Results from this work have been presented in over 45 presentations by project personnel including national conferences (e.g., American Chemical Society, American Geophysical Union, Clay Minerals Society, Goldschmidt Conference, Soil Science Society of America) and at invited academic seminars.

References

1. Steefel, C.I., S. Carroll, P.H. Zhao, and S. Roberts, *Cesium migration in Hanford sediment: a multisite cation exchange model based on laboratory transport experiments.* Journal of Contaminant Hydrology, 2003. **67**(1-4): p. 219-246.
2. Chorover, J., S. Choi, P. Rotenberg, R.J. Serne, N.A. Rivera, C. Strepka, A. Thompson, K.T. Mueller, and P.A. O'Day, *Silicon control of strontium and cesium partitioning in hydroxide-weathered sediments.* Geochim. Cosmochim. Acta, 2007: p. In press.
3. Mon, J., Y.J. Deng, M. Flury, and J.B. Harsh, *Cesium incorporation and diffusion in cancrinite, sodalite, zeolite, and allophane.* Microporous And Mesoporous Materials, 2005. **86**(1-3): p. 277-286.
4. Crosson, G., *Solid-State Nuclear Magnetic Resonance Studies of Hydroxide Promoted Dissolution of Layered Silicates*, in *Chemistry*. 2005, Pennsylvania State University: State College.
5. Crosson, G., S. Choi, J. Chorover, M.K. Amistadi, P.A. O'Day, and K.T. Mueller, *Solid-state NMR identification and quantification of newly formed aluminosilicate phases in weathered kaolinite systems.* Journal of Physical Chemistry B, 2006. **110**: p. 723-732.
6. Choi, S., P.A. O'Day, N.A. Rivera, K.T. Mueller, M.A. Vairavamurthy, S. Seraphin, and J. Chorover, *Strontium speciation during reaction of kaolinite with simulated tank-waste leachate: Bulk and microfocused EXAFS analysis.* Environmental Science & Technology, 2006. **40**: p. 2608-2614.
7. Chorover, J., S.K. Choi, M.K. Amistadi, K.G. Karthikeyan, G. Crosson, and K.T. Mueller, *Linking cesium and strontium uptake to kaolinite weathering in simulated tank waste leachate.* Environmental Science & Technology, 2003. **37**(10): p. 2200-2208.
8. Choi, S., M.K. Amistadi, and J. Chorover, *Clay mineral weathering and contaminant dynamics in a caustic aqueous system - I. Wet chemistry and aging effects.* Geochimica Et Cosmochimica Acta, 2005a. **69**(18): p. 4425-4436.
9. Choi, S., G. Crosson, K.T. Mueller, S. Seraphin, and J. Chorover, *Clay mineral weathering and contaminant dynamics in a caustic aqueous system - II. Mineral transformation and microscale partitioning.* Geochimica Et Cosmochimica Acta, 2005b. **69**(18): p. 4437-4451.
10. Crosson, G.S., S.Y. Choi, J. Chorover, M.K. Amistadi, P.A. O'Day, and K.T. Mueller, *Solid-state NMR identification and quantification of newly formed aluminosilicate phases in weathered kaolinite systems.* Journal of Physical Chemistry B, 2006. **110**(2): p. 723-732.
11. Fitz Gerald, J.D., J.B. Parise, and I.D.R. Mackinnon, *Average structure of an An48 plagioclase from the Hogarth Ranges.* American Mineralogist, 1986. **71**(11-12): p. 1399-1408.

12. Benna, P. and E. Bruno, *Single-crystal in situ high-temperature structural investigation on strontium feldspar.* American Mineralogist, 2001. **86**(5-6): p. 690-696.
13. Chorover, J., S. Choi, P. Rotenberg, R.J. Serne, and P.A. O'Day, *Coupling contaminant sorption and mineral transformation in Hanford sediments.* Geochimica et Cosmochimica Acta, in review.
14. Zhao, H.T., Y.J. Deng, J.B. Harsh, M. Flury, and J.S. Boyle, *Alteration of kaolinite to cancrinite and sodalite by simulated hanford tank waste and its impact on cesium retention.* Clays and Clay Minerals, 2004. **52**(1): p. 1-13.
15. Bowers, G.M., A.S. Lipton, and K.T. Mueller, *High-field QCPMG NMR of strontium nuclei in natural minerals.* Solid State Nuclear Magnetic Resonance, 2006. **29**(1-3): p. 95-103.
16. Bowers, G.M. and K.T. Mueller, *Electric field gradient distributions about strontium nuclei in cubic and octahedrally symmetric crystal systems.* Physical Review B, 2005. **71**(22): p. -.
17. Bowers, G.M., R. Ravella, S. Komarneni, and K.T. Mueller, *NMR study of strontium binding by a micaceous mineral.* Journal of Physical Chemistry B, 2006. **110**(14): p. 7159-7164.
18. Choi, S., P.A. O'Day, N.A. Rivera, K.T. Mueller, M.A. Vairavamurthy, S. Seraphin, and J. Chorover, *Strontium speciation during reaction of kaolinite with simulated tank-waste leachate: Bulk and microfocused EXAFS analysis.* Environmental Science & Technology, 2006. **40**(8): p. 2608-2614.
19. Choi, S.K., M.K. Amistadi, S. Seraphin, and J. Chorover, *Cesium and strontium uptake to clay minerals and their weathering products in a caustic waste.* Abstracts of Papers of the American Chemical Society, 2004. **227**: p. U1042-U1042.
20. Um, W. and R.J. Serne, *Iodide adsorption and transport at the Hanford Site, Washington.* Geochimica Et Cosmochimica Acta, 2005. **69**(10): p. A870-a870.
21. Um, W. and R.J. Serne, *Sorption and transport behavior of radionuclides in the proposed low-level radioactive waste disposal facility at the Hanford site, Washington.* Radiochimica Acta, 2005. **93**(1): p. 57-63.
22. Um, W., R.J. Serne, S.B. Yabusaki, and A.T. Owen, *Enhanced radionuclide immobilization and flow path modifications by dissolution and secondary precipitates.* Journal of Environmental Quality, 2005. **34**(4): p. 1404-1414.
23. Bostick, B.C., M.A. Vairavamurthy, K.G. Karthikeyan, and J. Chorover, *Cesium adsorption on clay minerals: An EXAFS spectroscopic investigation.* Environmental Science & Technology, 2002. **36**(12): p. 2670-2676.
24. Wan, J.M., T.K. Tokunaga, J.T. Larsen, and R.J. Serne, *Geochemical evolution of highly alkaline and saline tank waste plumes during seepage through vadose zone sediments.* Geochimica Et Cosmochimica Acta, 2004. **68**(3): p. 491-502.
25. Um, W., R.J. Serne, and K.M. Krupka, *Linearity and reversibility of iodide adsorption on sediments from Hanford, Washington under water saturated conditions.* Water Research, 2004. **38**(8): p. 2009-2016.
26. Chorover, J., P.A. Rotenberg, and R.J. Serne, *Mineral formation and radionuclide sorption in waste-impacted Hanford sediments.*, in *Proceedings of the 11th International Symposium on Water-Rock Interaction (WRI-11)*, R.B. Wanty, Editor. 2004: Saratoga Springs NY. p. 675-678.
27. Rotenberg, P.A., *Sediment Weathering and Contaminant Uptake in a Caustic Waste Simulant*, in *Soil Science Department*. 2003, Pennsylvania State University: University Park, PA.
28. Bowers, G.M., *Structural Investigations of Strontium in Inorganic Crystals, Organic Crystals, and Phyllosilicate Minerals with Strontium-87 NMR*, in *Chemistry Department*. 2006, Pennsylvania State University: University Park, PA.
29. Crosson, G., *Solid-State Nuclear Magnetic Resonance Studies of Hydroxide Promoted Dissolution of Layered Silicates*, in *Chemistry Department*. 2005, Pennsylvania State University: University Park, PA.